PROCEEDINGS OF SCIENCE

Reveiw of Belle QCD Results

Min-Zu Wang[*†]
Department of Physics, Institute of Astrophysics and
Leung Center for Cosmology and Particle Astrophysics,
National Taiwan University, Taiwan
E-mail: mwang@phys.ntu.edu.tw

Recent results of QCD interests from Belle are reported. These include the study of $e^+e^- \to \pi^+\pi^- J/\psi$, measurement of $e^+e^- \to \omega\pi^0$, $K^*(892)\bar{K}$ and $K_2^*(1430)\bar{K}$ at $\sqrt{s}$ near 10.6 GeV, and high-statistics study of K_S^0 pair production in two-photon collisions. The data samples used in these studies were collected by the Belle detector at or near the Υ resonances at the KEKB asymmetric energy e^+e^- (3.5 on 8 GeV) collider.

XXII International Europhysics Conference on High Energy Physics
18-24 July 2013
Stockholm, Sweden

[*]Speaker.
[†]on behalf of the Belle Collaboration

PoS(EPS-HEP 2013)467

1. Introduction

Quantum Chromodynamics (QCD) is the theory to describe the fundamental interactions between quarks and gluons which are the basic building blocks of hadrons. The hadron spectroscopy can offer valuable information to understand QCD. For example the exotic states like glue ball, tetraquark or four-quark molecule, etc. are useful to validate the lattice QCD calculations/predictions. The production cross section and the angular distribution of the energetic quark anti-quark pair in the fragmentation process as a function of the center-of-mass energy are also of general interests for the study of perturbative QCD. In this presentation, we will report recent results related to the above topics of QCD interests. The total data samples used are ~ 1 ab^{-1} collected by the Belle [1] detector at or near the Υ resonances at the KEKB [2] asymmetric energy e^+e^- (3.5 on 8 GeV) collider..

2. $e^+e^- \to \pi^+\pi^- J/\psi$ [3]

We use the the initial-state-radiation (ISR) process $e^+e^- \to \gamma_{\rm ISR}\pi^+\pi^- J/\psi$ to determine the production cross section of $e^+e^- \to \pi^+\pi^- J/\psi$ in the 3.5 GeV - 4.5 GeV region. The Belle data sample with an integrated luminosity of 967 fb^{-1} is used in this study. The PHOKHARA [4] event generator and GEANT [5] package are used to obtain the signal efficiency. Since there are four charged tracks in the final state, the trigger efficiency is good for observing this process. The ISR $\psi(2S)$ production rate is used to validate our cross section measurement. The corresponding cross sections are $(14.12\pm0.18\pm0.85)$ pb and $(15.13\pm0.11\pm0.79)$ pb at $\sqrt{s} = 10.58$ GeV for the e^+e^- and $\mu^+\mu^-$ modes, respectively, which agree within errors with the prediction of (14.25 ± 0.26) pb using the world-average resonance parameters [6].

Figure 1(a) shows the $\pi^+\pi^- l^+ l^-$ invariant mass distributions after some selection requirements [3] are applied. The background distribution is estimated with the normalized J/ψ-mass sidebands. We found that two Breit-Wigner (BW) functions with a relative phase can describe our data well. However, there are two equally good solutions in the fit.The resonance at higher mass is $Y(4260)$ which was first observed by BaBar and later confirmed by CLEO and Belle.

Since there are enough statistics, we select events near $Y(4260)$ peak and make projection plots. They are shown in Fig. 2. Clear peaks near 3.9 GeV/c^2 are observed in Fig. 2(b) and (c). The bumps in lower mass region of $M_{\pi^\pm J/\psi}$ can be identified as the reflection of the peak near 3.9 GeV/c^2. We perform an unbinned maximum likelihood fit to the distribution of $M_{\rm max}(\pi J/\psi)$, the maximum of $M(\pi^+ J/\psi)$ and $M(\pi^- J/\psi)$ in order to extract the information on the peak. The fit yields a mass of $(3894.5\pm6.6\pm4.5)$ MeV$/c^2$ and a width of $(63\pm24\pm26)$ MeV$/c^2$. This newly found resonance, i.e. charged charmonium-like state, is consistent with the findings reported in Ref. [7].

3. $e^+e^- \to \omega\pi^0$, $K^*(892)\bar{K}$, $K_2^*(1430)\bar{K}$ [8]

For a e^+e^- center-of-mass (CM) energy $\sqrt{s}$ much larger than resonance masses, the production cross sections of $\omega\pi^0 : K^*(892)^0\bar{K}^0 : K^*(892)^- K^+$ is expected to be 9:8:2 if SU(3) flavor symmetry is exact. However, this relation was found to be invalid at $\sqrt{s} = 3.67$ GeV and 3.773 GeV

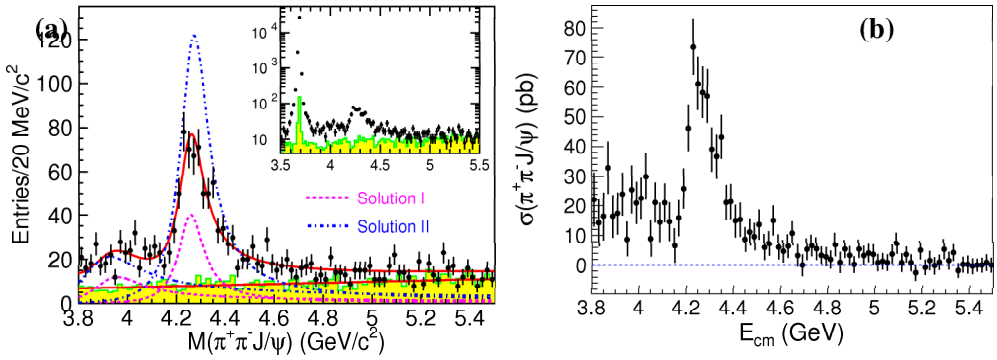

Figure 1: (a) Invariant mass distributions of $\pi^+\pi^- l^+ l^-$. Points with error bars are data, and the shaded histograms are the normalized J/ψ mass sidebands. The solid curves show the total best fit with two coherent resonances and contribution from background. The dashed curves are for solution I, while the dot-dashed curves are for solution II. The inset shows the distributions on a logarithmic vertical scale. The large peak around 3.686 GeV/c^2 is the $\psi(2S) \to \pi\pi J/\psi$ signal. (b) Cross section of $e^+e^- \to \pi^+\pi^- J/\psi$ after background subtraction. The errors are statistical only.

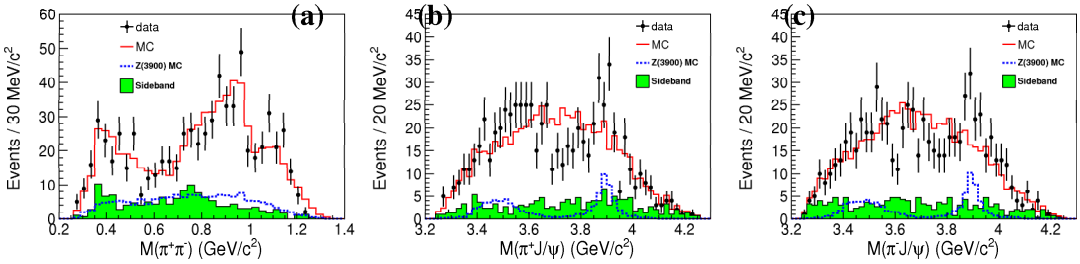

Figure 2: Invariant mass distributions of (a) $\pi^+\pi^-$, (b) $\pi^+ J/\psi$ and (c) $\pi^- J/\psi$ for events in the $Y(4260)$ signal region. Points with error bars represent data, shaded histograms are normalized background estimates from the J/ψ-mass sidebands, solid histograms represent MC simulations of $\pi^+\pi^-$ amplitudes (normalized J/ψ-mass sideband events added) and dashed histograms are MC simulation results for a $Z(3900)^\pm$ signal

.

by the CLEO experiment [9]. Based on a pQCD calculation [10] which takes $SU(3)_f$ symmetry breaking and the transverse momentum distribution of partons in the light cone wave functions of mesons into account, most of the CLEO measurements can be reproduced with reasonable input parameters. This calculation also predicts that $R_{VP} = 6.0$, where $R_{VP} = \frac{\sigma_B(e^+e^- \to K^*(892)^0 \bar{K}^0)}{\sigma_B(e^+e^- \to K^*(892)^- K^+)}$, and the cross sections of $e^+e^- \to$ vector-pseudoscalar (VP) vary as $1/s^3$.

We use the data samples of 89 fb^{-1}, 703 fb^{-1}, and 121 fb^{-1} collected at $\sqrt{s}$ =10.52, 10.58 ($\Upsilon(4S)$ peak), and 10.876 GeV ($\Upsilon(5S)$ peak), respectively, to study $e^+e^- \to \omega\pi^0$, $K^*(892)\bar{K}$, $K_2^*(1430)\bar{K}$. The Monte Carlo (MC) generator with next-to-leading order radiative corrections,MCGPJ, is used for signal simulation. We use PYTHIA [12] to estimate the background contributions from $e^+e^- \to u\bar{u}/d\bar{d}/s\bar{s}$.

An energy conservation variable $X_T = \Sigma_h E_h/\sqrt{s}$, where E_h is the energy of the final-state particle h in the e^+e^- CM frame is very useful to identify the signal candidates which should have a X_T value around 1. After applying the selection requirements described in Ref. [8], Figure 3 shows

the X_T distributions for $e^+e^- \to \pi\pi\pi^0\pi^0$ and $e^+e^- \to K^0_S K^+\pi^-$ with the $\Upsilon(4S)$ data set. We select the signal enriched region to make projection plots, shown in Fig. 4. Clear peaks for ω, $K^*(892)$ and $K^*_2(1430)$ are found. After applying the radiative corrections for different final states and the vacuum polarization factors at different s, we obtain the production cross sections at Born level for the measured processes and they are listed in Table 1. It is clear that the theoretical prediction for $R_{\rm VP} = 6.0$ is definitely violated. This violation is also found in another study using $\Upsilon(1S)$ and $\Upsilon(2S)$ samples at Belle [13]. Combining the CLEO and Belle measurements, the production cross section seems to match $1/s^4$ better than the predicted $1/s^3$ trend. Figure 5 is an illustration with $e^+e^- \to K^*(892)^0\bar{K}^0$.

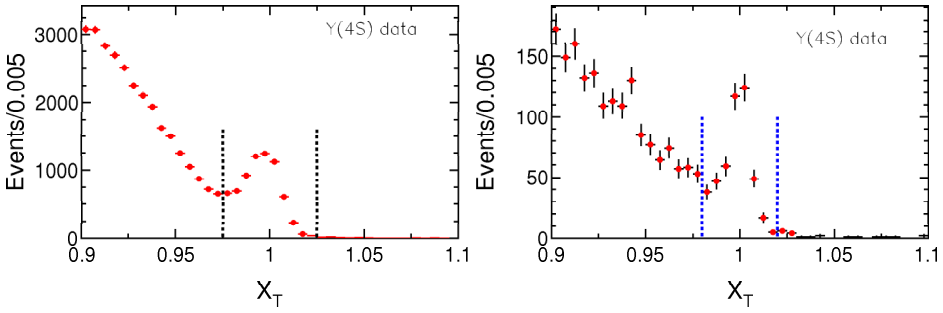

Figure 3: The scaled total energy X_T distributions for the selected $e^+e^- \to \pi\pi\pi^0\pi^0$ (left) and $K^0_S K^+\pi^-$ (right) candidate events from the $\sqrt{s} = 10.58$ GeV data sample. The signal region is indicated between the dotted lines.

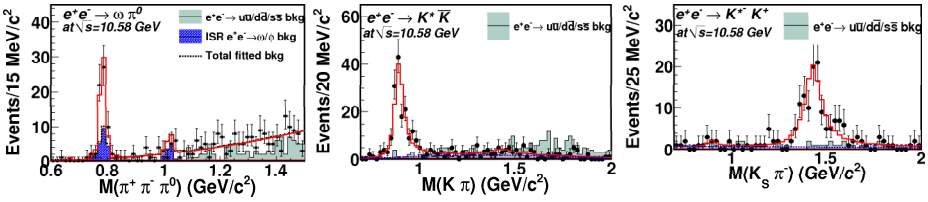

Figure 4: Fits to the $\pi^+\pi^-\pi^0$ (left), $K^+\pi^-$ (middle) and $K^0_S\pi^-$(right) mass distributions with candidate events in the signal region for the $\sqrt{s} = 10.58$ GeV data sample. The solid lines show the fit results, the dotted curves show the total estimated background, the dark shaded histograms are from the normalized ISR backgrounds $e^+e^- \to \gamma_{\rm ISR}\omega/\phi \to \gamma_{\rm ISR}\pi^+\pi^-\pi^0$ and the light shaded histograms are from the normalized $e^+e^- \to u\bar{u}/d\bar{d}/s\bar{s}$ backgrounds. The dotted curves are not significantly seen in the signal regions due to low background level.

4. $\gamma\gamma \to K^0_S K^0_S$[14]

We study of the cross section for $\gamma\gamma \to K^0_S K^0_S$ in the W region from $K^0_S K^0_S$ mass threshold up to 4.0 GeV and in the angular range $|\cos\theta^*| \leq 0.8$, where W is the total energy of the parent photons and θ^* is the scattering angle of the K^0_S in their CM frame, using a Belle data sample corresponding to an integrated luminosity of 972 fb^{-1}. The MC event generator, TREPS [17], is used for signal simulation. We use data to estimate different backgrounds. For example, the $\pi^+\pi^-$

Table 1: Results for the Born cross sections, where $N_{\rm sig}$ is the number of fitted signal events, $N_{\rm sig}^{\rm UL}$ is the upper limit on the number of signal events, ε is the efficiency, Σ is the signal significance, σ_B is the Born cross section, $\sigma_B^{\rm UL}$ is the upper limit on the Born cross section. All the upper limits are given at the 90% C.L. The first uncertainty in σ_B is statistical, and the second systematic.

Channel	$\sqrt{s}$ (GeV)	$N_{\rm sig}$	$N_{\rm sig}^{\rm UL}$	ε (%)	Σ (σ)	σ_B (fb)	$\sigma_B^{\rm UL}$ (fb)
$\omega\pi^0$	10.52	$4.1^{+3.3}_{-2.6}$	9.9	1.25	1.6	$4.53^{+3.64}_{-2.88}\pm0.50$	11
	10.58	$38.8^{+8.3}_{-7.6}$	—	1.10	6.7	$6.01^{+1.29}_{-1.18}\pm0.57$	—
	10.876	$-0.7^{+2.9}_{-2.1}$	7.0	1.07	—	$-0.68^{+2.71}_{-1.97}\pm0.20$	6.5
$K^*(892)^0\bar{K}^0$	10.52	$34.6^{+6.9}_{-6.1}$	—	16.49	7.4	$10.77^{+2.15}_{-1.90}\pm0.77$	—
	10.58	187 ± 17	—	16.30	>10	$7.48\pm0.67\pm0.51$	—
	10.876	$34.6^{+7.5}_{-6.7}$	—	17.25	7.2	$7.58^{+1.64}_{-1.47}\pm0.63$	—
$K^*(892)^-K^+$	10.52	$4.6^{+3.6}_{-2.7}$	9.3	20.40	1.4	$1.14^{+0.90}_{-0.67}\pm0.15$	2.3
	10.58	$5.9^{+4.7}_{-3.8}$	14	21.03	1.5	$0.18^{+0.14}_{-0.12}\pm0.02$	0.4
	10.876	$1.6^{+3.9}_{-3.0}$	8.5	21.29	0.3	$0.28^{+0.68}_{-0.52}\pm0.10$	1.5
$K_2^*(1430)^0\bar{K}^0$	10.52	$1.3^{+4.3}_{-3.9}$	6.8	17.63	0.3	$0.76^{+2.53}_{-2.26}\pm0.14$	4.0
	10.58	21^{+11}_{-10}	40	16.71	2.1	$1.65^{+0.86}_{-0.78}\perp0.27$	3.1
	10.876	$1.0^{+4.5}_{-3.7}$	8.9	19.02	0.2	$0.38^{+1.79}_{-1.47}\pm0.07$	3.5
$K_2^*(1430)^-K^+$	10.52	$12.0^{+6.2}_{-5.8}$	21	20.36	2.1	$6.06^{+3.13}_{-2.93}\pm1.34$	11
	10.58	129 ± 15	—	20.17	>10	$8.36\pm0.95\pm0.62$	—
	10.876	$17.6^{+5.3}_{-4.6}$	—	21.50	4.5	$6.20^{+1.86}_{-1.63}\pm0.64$	—

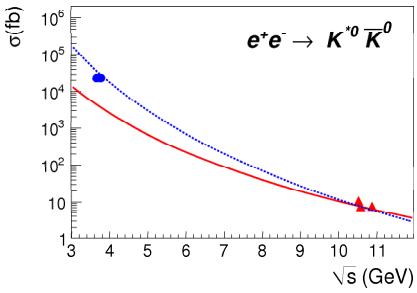

Figure 5: The cross sections for $e^+e^- \to K^{*0}(892)\bar{K}^0$. The data at $\sqrt{s} = 10.52$ GeV, 10.58 GeV, and 10.876 GeV are from our measurements. The data at $\sqrt{s} = 3.67$ GeV and 3.77 GeV, where shown, are from CLEO measurement [9]. Here, the uncertainties are the sum of the statistical and systematic uncertainties in quadrature. Upper limits are shown by the arrows. The solid line corresponds to a $1/s^3$ dependence and the dashed line to a $1/s^4$ dependence; the curves pass through the measured cross section at $\sqrt{s} = 10.58$ GeV.

background can be determined from the K_S^0 mass sideband. The non-exclusive process, $K_S^0K_S^0X$, can be estimated by fitting the p_t-balance ($|\sum\vec{p}_t^{\,*}|$) distribution with a function in which both the signal and background are considered. The trigger information and event selection requirements are described in Ref. [14].

Figure 6 shows the measured cross sections and systematic uncertainties as a function of W. There are many resonance-like structures found. We perform a partial-wave analysis to study the properties of these resonances. It is clear that the observed $f_0(1710)$ and $f_2(2200)$ are unlikely to be pure glueball states because their $\Gamma_{\gamma\gamma}$, two γ partial width, values are too large. We also study

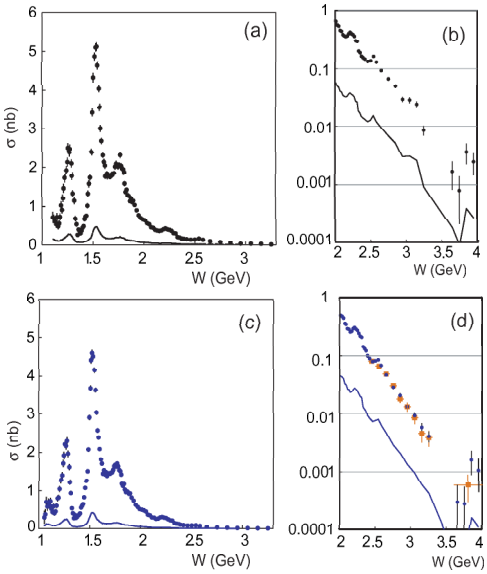

Figure 6: The W dependence of the $\gamma\gamma \to K^0_S K^0_S$ cross section after integrating over the angle up to (a,b) $|\cos\theta^*| < 0.8$ (black points) and (c,d) $|\cos\theta^*| < 0.6$ (blue points). The orange square markers in (d) are from our previous publication [15] for $|\cos\theta^*| < 0.6$. The solid curves are the systematic uncertainties.

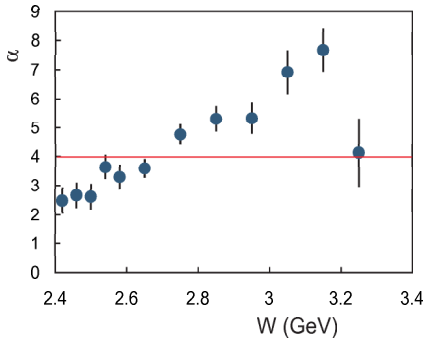

Figure 7: W dependence of the parameter α, which characterizes the angular dependence of the differential cross section. The horizontal line at $\alpha = 4$ corresponds to the claim of the handbag model.

the angular distribution with the form $\sim 1/\sin^{\alpha}\theta^*$ and obtain the W dependence of α, shown in Fig. 7. The handbag model [18] gives α a constant value at 4.

The W dependence of the $\gamma\gamma \to K^0_S K^0_S$ cross section is of general interests. We fit the cross section with a functional form $\sim W^{-n}$, where n is the slope parameter. Figure 8 shows the value is between 10 and 11 which is much larger than 6 and 7 that are observed for the $\pi^+\pi^-$ and K^+K^- processes. For the theoretical investigation in Refs. [19, 20], the pQCD calculation gives a $n = 10$ prediction for $\gamma\gamma \to K^0_S K^0_S$. It agrees reasonably well with our present measurement.

Acknowledgments

The author wish to thank the KEKB accelerator group for the excellent operation of the KEKB accelerator. This work is supported by the National Science Council of the Republic of China under

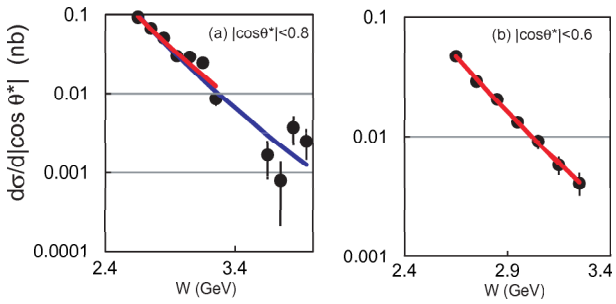

Figure 8: Results for the cross section integrated over $|\cos\theta^*|$ regions (a) below 0.8 and (b) below 0.6. The W dependence is fitted to W^{-n} in the different W regions: 2.6 – 4.0 GeV except 3.3 – 3.6 GeV (blue line) and 2.6 – 3.3 GeV (red line).

the grant NSC-99-2112-M-002-006-MY3.

References

[1] A. Abashian *et al.* (Belle Collaboration), Nucl. Instr. and Meth. A**479**, 117 (2002).

[2] S. Kurokawa and E. Kikutani, Nucl. Instr. and Meth. A**499**, 1 (2003) and other papers included in this Volume.

[3] Z.Q. Liu *et al.* (Belle Collaboration), Phys. Rev. Lett. **110** , 252002 (2013).

[4] G. Rodrigo, H. Czyż, J. H. Kühn and M. Szopa, Eur. Phys. J. C **24**, 71 (2002).

[5] R. Brun *et al.*, GEANT 3.21, CERN Report DD/EE/84-1, 1984.

[6] J. Beringer *et al.* (Particle Data Group), Phys. Rev. D **86** , 010001 (2012).

[7] M. Ablikim *et al.* (BESIII Collaboration), Phys. Rev. Lett. **110** , 252001 (2013).

[8] C.P. Shen *et al.* (Belle Collaboration), Phys. Rev. D**88**, 052019 (2013).

[9] N. E. Adam *et al.* (CLEO Collaboration), Phys. Rev. Lett. **94**, 012005 (2005); G. S. Adams *et al.* (CLEO Collaboration), Phys. Rev. D **73**, 012002 (2006).

[10] C. D. Lü, W. Wang and Y. M. Wang, Phys. Rev. D **75**, 094020 (2007).

[11] A. B Arbuzov *et al.*, JHEP **9710**, 001 (1997); A. B Arbuzov *et al.*, JHEP **9710**, 006 (1997); A. B. Arbuzov *et al.*, Eur. Phys. J. C **46**, 689 (2006); S. Actis *et al.*, Eur. Phys. J. C **66**, 585 (2010).

[12] T. Sjöstrand, S. Mrenna and P. Skands, JHEP **0605**, 026 (2006).

[13] C.P. Shen *et al.* (Belle Collaboration), Phys. Rev. D**88**, 011102 (2013).

[14] S. Uehara *et al.* (Belle Collaboration), arXiv:1307.7457, accepted by *Prog. Theor. Exp. Phys.*.

[15] W.T. Chen *et al.* (Belle Collaboration), Phys. Lett. B **651**, 15 (2007).

[16] S. Uehara, Y. Watanabe *et al.* (Belle Collaboration), Phys. Rev. D **78**, 052004 (2008).

[17] S. Uehara, KEK Report 96-11 (1996).

[18] M. Diehl, P. Kroll and C. Vogt, Phys. Lett. B **532**, 99 (2002).

[19] V.L. Chernyak, Phys. Lett. B **640**, 246 (2006).

[20] V.L. Chernyak, arXiv 1212.1304 [hep-ph]; contributed to "Workshop on QCD in two-photon processes", 2 - 4 October 2012, Taipei.